Tribology International 42 (2009) 303–310

Contents lists available at ScienceDirect

Tribology International

journal homepage: www.elsevier.com/locate/triboint

Externally pressurized gas bearings: A comparison between two supply holes configurations

F. Colombo *, T. Raparelli, V. Viktorov

Department of Mechanics, Politecnico di Torino, C.so Duca degli Abruzzi 24, Torino, Italy

ARTICLE INFO

Article history:
Received 19 February 2007
Received in revised form
29 January 2008
Accepted 24 June 2008
Available online 8 August 2008

Keywords:
Journal bearings
Lubrication
High speed

ABSTRACT

Radial vibration of a vertical rotor with externally pressurized gas bearings is analyzed. The time-dependent Reynolds equation is solved together with the journal equation of motion to obtain the response characteristics of the bearing system. The bearings are supplied with either one or two sets of supply orifices. Stiffness and flow rate are compared for both cases. Stability maps are obtained at different supply pressures and with different supply orifice diameters. The mass range from orbital stability to instability is studied as a function of supply hole downstream pressure level.

1. Introduction

Though gas bearings can be a preferred solution in high-speed applications because of their low friction and wear, a major problem encountered in designing this kind of bearing is that of self-excited instability. Numerous studies have been conducted of self-acting bearings and pressurized bearings, taking different approaches to this problem. The linear theory is widely used to predict rotor trajectories and stability in bearing systems because of its simplicity [1–4]. In [4], the linear perturbation method, used to compute the stiffness and damping coefficients, is compared with a nonlinear analysis for noncircular bearings. It is demonstrated that the linearized solution agrees well with the small amplitude orbit, but is unable to predict the orbits with larger amplitudes, especially as regards the large unbalance response. The difference between the whirl loci under large dynamic excitations predicted by the linear and nonlinear theories is presented in [5].

In [6] is described Hopf bifurcation, which takes place for overcritical masses of the rotor, when the static equilibrium position of rotor is lost. It appears with stable limit cycles, whose amplitude depends strongly on the mass. The same author in [7] presents an interesting method to obtain stiffness and damping coefficients of gas bearings in order to predict resonance vibrations and the amplitude of unbalanced vibrations. In [8,9] is shown an elastic supporting structure between the bearing bushes and the casing that makes it possible to retain steady-state stability at any rotational velocity. This can be obtained with properly selected stiffness and damping coefficients of the elastic bush support.

To determine the nonlinear behavior of externally pressurized bearings and plot stability diagrams at different supply pressures, the investigation described herein numerically integrated the time-dependent nonlinear Reynolds equation together with the rotor equations of motion in the radial vibration mode for a rotor-air-bearing system, with the rotor in vertical attitude. Radial bearings with $L/D = 1$ were considered with a 30 mm diameter rotor positioned symmetrically with respect to the bearings.

The study considered two externally pressurized-bearing geometries: one with four supply holes in the mid-plane, and one with two sets of supply holes. The two geometries were compared as regards their stiffness, air consumption and stability.

For the second geometry, a further, in-depth study was conducted of how the orbit amplitude varies with the rotor mass at different supply hole downstream pressure levels.

2. Mathematical model

The system investigated herein consists of a vertical rigid axial-symmetric rotor supported by two bushings positioned symmetrically with respect to the rotor center of mass. The rotor-bearing system's equations of radial motion are

$$m\ddot{x} = F_{ex} + F_{px} + F_{fx}$$
$$m\ddot{y} = F_{ey} + F_{py} + F_{fy} \quad (1)$$

* Corresponding author. Fax: +390 110 906 999.
E-mail address: federico.colombo@polito.it (F. Colombo).

0301-679X/$ - see front matter © 2008 Elsevier Ltd. All rights reserved.
doi:10.1016/j.triboint.2008.06.014

Nomenclature

Symbols

b	ratio of critical pressure to admission pressure
c_d	discharge coefficient of the supply orifice
c_s	conductance of the supply orifice
d_s	diameter of the supply orifice
D	diameter of shaft
e	radial journal centre displacement
F_e	external bearing load
F_f	friction force
F_p	pressure force
h	film thickness
h_0	journal bearing average radial clearance
K	rotor angular moment
k_T	$\sqrt{293/T^0}$, temperature coefficient, where T_0 is absolute temperature in normal condition
L	length of bearing
m	mass of shaft
n	angular speed of rotor, rpm
p	pressure
p_c	downstream static pressure at supply orifice
Q_s	mass flow rate at supply orifice
q	mass flow rate per unit surface
R	radius of shaft
R^0	gas constant, in calculations $R^0 = 287.6\,\mathrm{m^2/s^2\,K}$
r	radial coordinate
S_s	output surface of supply chamber
T^0	absolute temperature, in calculations 288 K
W	a dimensional stiffness parameter
t	time
x, y, z	cartesian coordinates
α	coefficient in stability parameter
β	coefficient in stability parameter
γ	v/ω, whirl ratio
ε	e/h_0, eccentricity ratio
θ	angular coordinate
Λ_L	$(L/D)^2\,\Lambda_R$
Λ_R	$(6\mu\omega/p_a)(R/h_0)^2$, bearing number
Ψ	$0.685/(R^0T^0)^{-0.5}$ constant in calculation of conductance
μ	dynamic viscosity
v	whirling angular speed of rotor center (rad/s)
ρ	density
ω	angular speed of rotor (rad/s)

Subscripts

a	ambient
N	normal condition
s	supply
x	x-component
y	y-component

where F_p and F_f are due, respectively, to pressure and viscous tangential actions.

Film thickness is given by

$$h = h_0 - e_x \cos\vartheta - e_y \sin\vartheta \tag{2}$$

The complete Reynolds equation for compressible fluid is solved in a range in which inertial effects are negligible. In fact, $Re^* = \rho\omega(h_0^2/\mu) < 0.34$ and [10] demonstrates that inertial effects are negligible up to $Re^* = 1$:

$$\frac{\partial}{\partial z}\left(ph^3\frac{\partial p}{\partial z}\right) + \frac{\partial}{r\partial\vartheta}\left(ph^3\frac{\partial p}{r\partial\vartheta}\right) + 12\mu R^0T^0q = 6\mu\omega\frac{\partial(ph)}{\partial\theta} + 12\mu\frac{\partial(ph)}{\partial t} \tag{3}$$

The mass flow rate per unit surface at supply orifice is $q = Q_s/r\,\mathrm{d}\theta\,\mathrm{d}z$, where Q_s is defined by the equation

$$Q_s = c_s k_T \rho_N p_s \sqrt{1 - \left(\frac{(p/p_s) - b}{1 - b}\right)^2} \tag{4}$$

according to the ISO formula for flow rate through a hole (ISO 6358, 1989) [11,12].

The conductance c_s, as defined in [13], is

$$c_s = c_d \frac{\pi d_s^2}{4} \frac{0.6855}{\rho_N \sqrt{R^0 T^0}} \tag{5}$$

where the discharge coefficient c_d is assumed to be independent on the local clearance and equal to 0.8.

The system of equations is solved by finite difference Euler explicit method.

The integration grid for one bearing has 25 nodes in the axial direction and 96 in the circumferential direction in order to describe the pressure distribution with an acceptable degree of approximation (error <3%).

3. Conductance analysis

Two different kinds of bearings are analyzed (Fig. 1), both with a diameter of 30 mm, ratio $L/D = 1$ and clearance $h_0 = 20\,\mu$m. The first geometry considered (bearing 1) features four supply holes in the center plane, while the second (bearing 2) features two sets of supply holes situated on planes at $z = L/4$ and $3/4L$.

In [11], it was shown that the hole downstream pressure level p_{c0} calculated with the shaft in the central position and with $\Lambda = 0$ is an important parameter that influences the stability of externally pressurized bearings. This parameter depends on the diameter d_s of the supply holes, on their arrangement if the holes are adjacent, on clearance h_0 and on supply pressure p_s.

The dynamic behavior of bearings with different hole diameters can be compared if the hole downstream pressure level p_{c0} is the same. For this purpose, an analysis of the resistances at different supply pressures with the shaft in the central position was performed under both static and rotating conditions. A schematic view of the supply system is shown in Fig. 2.

The Reynolds equation was solved for fixed geometry and with the initial condition $p = p_a$ at all points to find the steady-state solution. Multiple iterations were carried out in order to find the

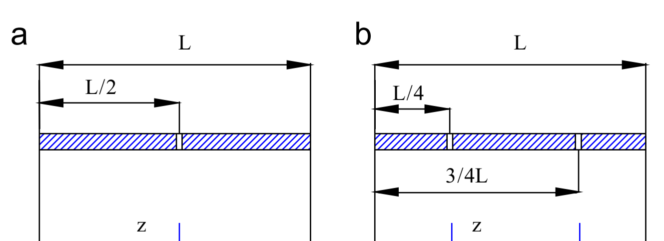

Fig. 1. Bearing geometries considered: (a) geometry 1, bearing with one row of holes and (b) geometry 2, bearing with two rows of holes.